



# Clinical features and neuroimaging (CT and MRI) findings in presumed Zika virus related congenital infection and microcephaly: retrospective case series study

Maria de Fatima Vasco Aragao,<sup>1</sup> Vanessa van der Linden,<sup>2</sup> Alessandra Mertens Brainer-Lima,<sup>3</sup> Regina Ramos Coeli,<sup>4</sup> Maria Angela Rocha,<sup>4</sup> Paula Sobral da Silva,<sup>4</sup> Maria Durce Costa Gomes de Carvalho,<sup>4</sup> Ana van der Linden,<sup>5</sup> Arthur Cesario de Holanda,<sup>6</sup> Marcelo Moraes Valenca<sup>7</sup>

<sup>1</sup>Centro Diagnostico Multimagem, Rua Frei Matias Tevis, 194, Ilha do Leite Recife Pernambuco 52010-450, Brazil; Medical School, Mauricio de Nassau University, Recife, Pernambuco, Brazil

<sup>2</sup>Association for Assistance of Disabled Children, Recife, Brazil; Barão de Lucena Hospital, Recife, Brazil

<sup>3</sup>PROCAPE, University of Pernambuco, Recife, Brazil

<sup>4</sup>Oswaldo Cruz University Hospital, Recife, Brazil

<sup>5</sup>Prof Fernando Figueira Integral Medicine Institute, Recife, Brazil

<sup>6</sup>Medical School, Federal University of Pernambuco, Recife, Brazil

<sup>7</sup>Neurology and Neurosurgery, Federal University of Pernambuco, Recife, Brazil

Correspondence to: M de Fatima Vasco Aragao fatima.vascoaragao@gmail.com

Cite this as: *BMJ* 2016;353:i1901 <http://dx.doi.org/10.1136/bmj.i1901>

Accepted: 1 April 2016

## ABSTRACT

### OBJECTIVE

To report radiological findings observed in computed tomography (CT) and magnetic resonance imaging (MRI) scans of the first cases of congenital infection and microcephaly presumably associated with the Zika virus in the current Brazilian epidemic.

### DESIGN

Retrospective study with a case series.

### SETTING

Association for Assistance of Disabled Children (AACD), Pernambuco state, Brazil.

### PARTICIPANTS

23 children with a diagnosis of congenital infection presumably associated with the Zika virus during the Brazilian microcephaly epidemic.

### MAIN OUTCOME MEASURES

Types of abnormalities and the radiological pattern of lesions identified on CT and MRI brain scans.

### RESULTS

Six of the 23 children tested positive for IgM antibodies to Zika virus in cerebrospinal fluid. The other 17 children met the protocol criteria for congenital infection presumably associated with the Zika virus, even without being tested for IgM antibodies to the virus—the test was not yet available on a routine basis. Of the 23 children, 15 underwent CT, seven underwent both CT and MRI, and one underwent MRI. Of the 22 children who underwent CT, all had calcifications in the junction between cortical and subcortical white matter, 21 (95%) had malformations of cortical development, 20 (91%) had a decreased brain volume, 19 (86%) had ventriculomegaly, and 11 (50%) had hypoplasia of the cerebellum or brainstem. Of the eight children who underwent MRI, all had

calcifications in the junction between cortical and subcortical white matter, malformations of cortical development occurring predominantly in the frontal lobes, and ventriculomegaly. Seven of the eight (88%) children had enlarged cisterna magna, seven (88%) delayed myelination, and six each (75%) a moderate to severe decrease in brain volume, simplified gyral pattern, and abnormalities of the corpus callosum (38% hypogenesis and 38% hypoplasia). Malformations were symmetrical in 75% of the cases.

### CONCLUSION

Severe cerebral damage was found on imaging in most of the children in this case series with congenital infection presumably associated with the Zika virus. The features most commonly found were brain calcifications in the junction between cortical and subcortical white matter associated with malformations of cortical development, often with a simplified gyral pattern and predominance of pachygyria or polymicrogyria in the frontal lobes. Additional findings were enlarged cisterna magna, abnormalities of corpus callosum (hypoplasia or hypogenesis), ventriculomegaly, delayed myelination, and hypoplasia of the cerebellum and the brainstem.

## Introduction

Since October 2015 there has been an increase in the number of children with microcephaly in Pernambuco,<sup>1</sup> a Brazilian state with nine million inhabitants. Several possible explanations for this phenomenon have been proposed, including an association with the current rise in Zika virus infections observed since March 2015.<sup>1</sup>

The putative association between Zika virus infection in mothers during pregnancy and microcephalic offspring is based on epidemiological and laboratory evidence. These include the temporal association between the Zika virus epidemic and concomitant increase in the number of babies born with microcephaly<sup>1</sup>; the identification of the Zika virus genome (using reverse transcription-polymerase chain reaction assay) in amniotic fluid samples from two pregnant women with microcephalic fetuses<sup>2</sup>; the detection of the Zika virus genome in the blood and tissue samples of a newborn baby with microcephaly who died five minutes after birth<sup>3</sup>; the demonstration of Zika virus neurotropism in experimental animals<sup>4</sup>; the discovery that Zika virus can cause death of neural cells<sup>5</sup>; and the finding of a higher frequency of abnormalities detected by ultrasonography in pregnant women with Zika virus infection compared with those without.<sup>6</sup>

## WHAT IS ALREADY KNOWN ON THIS TOPIC

Radiological findings characteristic of infants with congenital Zika virus related microcephaly have been not been well characterised

## WHAT THIS STUDY ADDS

The radiological pattern of children with a diagnosis of presumed congenital Zika virus related infection was characterised by brain calcifications at the junction between cortical and subcortical white matter associated with other malformations of cortical development

Other common findings were better visualised using magnetic resonance imaging. These findings were an enlarged cisterna magna, abnormalities of the corpus callosum (hypoplasia or hypogenesis), and cerebellum and brainstem hypoplasia

Zika virus is transmitted through the bite of an infected arthropod. The virus has been isolated from several species of mosquitoes: *Aedes africanus*, *Aedes luteocephalus*, and *Aedes aegypti*.<sup>7</sup> The last of these is also known to transmit other diseases, such as dengue and yellow fever, which are endemic infections, and Chikungunya, which has also emerged recently.<sup>3 8-10</sup> Zika virus epidemics have been described in several countries, especially in the most densely populated cities of tropical and subtropical regions.<sup>3 8-10</sup> Although Zika virus was first described in 1947,<sup>3 11</sup> no relation between Zika virus infection and microcephaly was confirmed until November 2015 in Brazil (table 1).<sup>2</sup> Epidemiological data suggest that cases of microcephaly in Brazil might be associated with the introduction of Zika virus.<sup>1</sup> This hypothesis was strongly supported in November 2015 by laboratory evidence from the amniotic fluid of women with microcephalic fetuses.<sup>1</sup> In February 2016, the World Health Organization declared Zika virus a global health emergency.<sup>16</sup>

Of the 5280 notified cases of microcephaly in Brazil up to 13 February 2016 (fig 1), only 1345 have been investigated and classified. Of these, Zika virus infection has been diagnosed in 508, according to the definitions of the Brazilian Ministry of Health's protocol. In Pernambuco, the state with most notifications (n=1544), 182 cases have been investigated and confirmed as presumed Zika virus related infection.<sup>17</sup>

Even though microcephaly is the principal characteristic of a severe congenital infection during the early stages of pregnancy, to the best of our knowledge, the radiological features of children with presumed Zika virus related congenital infection or microcephaly have not been well characterised. A case series from Brazil described the computed tomography (CT) and transfontanellar cranial ultrasound characteristics of Zika virus related microcephaly, but the images were not shown. The features on magnetic resonance imaging (MRI) have not been described in children born with microcephaly.<sup>18</sup> We describe the brain imaging (CT and MRI) features as well as principal clinical findings of children with microcephaly and presumed congenital infection related to the Zika virus during the epidemic in Pernambuco, Brazil.

## Patient involvement

No patients were involved in setting the research question or the outcome measures, nor were they involved in developing plans for design or implementation of the study. No patients were asked to advise on interpretation or writing up of results. There are no plans to disseminate the results of the research to study participants or the relevant patient community.

## Methods

This is a retrospective report of a case series of 23 children with microcephaly and presumed Zika virus related congenital infection during the Brazilian epidemic, 2015-16.

Since October 2015, health services and professionals in Pernambuco report all infants born in the state with suspected microcephaly on a government website (cievs.com/microcefalia). In the initial stages of the epidemic, microcephaly was defined as a head circumference of 33 cm or less. On 2 December 2015 the criterion for diagnosis changed to 32 cm or less for infants of gestational age 37 weeks or more, or, for preterm infants, 2 standard deviations below the mean for age and sex on the Fenton curve.

According to the Brazilian Ministry of Health's protocol, all infants born with suspected microcephaly in Pernambuco should be referred to one of two paediatric infectious disease departments and to one of four rehabilitation centres. The Association for Assistance of Disabled Children (AACD) is one of the rehabilitation centres. All investigations described in this report were conducted as part of the routine clinical evaluation of these children as established by clinical protocols defined by the Brazilian Ministry of Health and the health secretary of Pernambuco state,<sup>1</sup> and the differential diagnosis was based on clinical presentation, personal and family history, laboratory test results, and radiological findings. Parents or guardians gave consent before the procedures.

In AACD, all children are initially examined by a neurologist or physician specialising in physical medicine and rehabilitation, and, as needed, an ophthalmologist, orthopaedic consultant, and a multidisciplinary team of rehabilitation specialists. All children undergo

**Table 1 | Brief history of Zika virus epidemic and its association with microcephaly**

Period	Locations	Details
1947	Zika forest, Uganda, Africa	Zika virus described and isolated from a Rhesus monkey <sup>3 11</sup>
1952	Uganda, Africa	Zika virus reported in humans <sup>11</sup>
1951-81	South East Asia and sub-Saharan Africa	Sporadic cases of Zika virus infection <sup>3 11 12</sup>
2007	Yap Island, Micronesia	Outbreak of Zika virus infection <sup>3 11</sup>
2013-14	French Polynesia, New Caledonia, Cook Island, Easter Island	Outbreak of Zika virus infection, with two reported cases of perinatal transmission causing mild disease <sup>3 13</sup>
March 2015	Camaçari, Bahia, north east Brazil	Outbreak of Zika virus infection <sup>14</sup>
October 2015	Pernambuco, north east Brazil	Unexplained increase in microcephaly cases <sup>1</sup>
17 November 2015	Paraíba, north east Brazil	Zika virus genome detected through reverse transcriptase-polymerase chain reaction of amniotic fluid samples from two pregnant women with microcephalic fetuses <sup>2</sup>
24 November 2015	French Polynesia	Increase in malformations involving the central nervous system (including microcephaly) in newborn babies registered during 2014 and 2015 and conceived during the Zika virus outbreak in this area <sup>13-15</sup>
28 November 2015	Brazil	Zika virus genome detected in the blood and tissue samples of a newborn baby with microcephaly who died five minutes after birth <sup>1</sup>



Fig 1 | Map of Brazil showing cities with notified cases of microcephaly in Brazil up to 13 February 2016. Adapted from Brazilian Ministry of Health<sup>17</sup>

a CT brain scan without contrast. Some also undergo MRI of the brain, based on the results of the clinical evaluation, mainly the presence of refractory seizures or suspicion of hydrocephalus and arthrogryposis.

We used a standard form to collect personal and clinical data. Mothers gave information on illness during pregnancy compatible with Zika virus infection (eg, maculopapular rash, fever, headache, myalgia, arthralgia, and conjunctivitis), with or without serological confirmation, as well as any neurological dysfunction or craniofacial disproportion in the newborn.

The main agents of congenital infections that cause brain calcifications and microcephaly (cytomegalovirus, toxoplasmosis, rubella, and syphilis) were investigated with paired serology (IgM and IgG antibodies to Zika virus) of both mother and newborn. If IgG antibodies to cytomegalovirus were present in both, polymerase chain reaction was conducted on urine samples. We excluded from the study those children with known causes of microcephaly other than Zika virus. Cerebrospinal fluid samples from six children were tested by IgM antibody capture enzyme-linked immunosorbent assay (the new specific test for Zika virus), following the protocol of the Centers for Disease Control and Prevention.<sup>19</sup> Genetic testing is not included in the Brazilian government's protocol, and differential diagnosis is performed based on family history and imaging findings, as is done with all metabolic diseases. Other causes of microcephaly, such as prenatal and perinatal

complications and exposure to licit and illicit drugs, toxic substances, and ionising radiation were excluded in the children.

Children included in this report had microcephaly or craniofacial disproportion (diagnosed by ultrasound examination during pregnancy or at birth), or both; brain imaging suggestive of congenital infection; and negative test results for other known infectious causes of microcephaly (eg, toxoplasmosis, cytomegalovirus, rubella, syphilis, and HIV).

### CT and MRI scans

According to the protocol of the Brazilian government, all children with microcephaly undergo non-contrast brain CT after clinical examination. MRI is not included in the protocol, but it is performed when available, based on clinical indication. The evaluation of the images was exclusively qualitative.

All CT scanning was performed using a multislice CT scanner without contrast, and all MRI was performed using a 1.5T MRI scanner. Only in one child was MRI done with contrast. The conventional MRI sequences available for analysis were T1 weighted imaging, T2 weighted imaging, susceptibility magnetic weighted imaging or T2\* gradient echo, and diffusion weighted imaging.

We reviewed the CT scans for decreased brain volume; cerebral ventricular enlargement due to white matter hypoplasia, associated with or without communicating hydrocephalus; malformations of cortical development, and sulcation; the presence and location of brain calcifications; decreased cerebellum and brainstem volume; enlarged cisterna magna; and enlarged anterior supratentorial subarachnoid space.

We reviewed the MRI scans for decreased brain volume, classified as mild (grade I), moderate (grade II), or severe (grade III); cerebral ventricular enlargement due to white matter hypoplasia; malformations of cortical development and sulcation; abnormalities of the corpus callosum (classified as agenesis, hypogenesis, and hypoplasia); evaluation of myelination (normal or delayed); presence and location of brain calcifications; decreased brainstem and cerebellum volume; enlarged cisterna magna; enlarged anterior supratentorial subarachnoid space; and presence of intraparenchymal cysts. The criteria for assessment of myelination were based on a previous study,<sup>20</sup> where the authors charted the ages at which changes in myelination appear on T1 and T2 weighted images, as well as the normal milestones for brain myelination. We considered mainly T1 weighted images as the most useful sequence for assessing normal brain maturation in children during the first six months. T1 and T2 weighted images were available for all the children, except one, who underwent only T2 weighted imaging.

### Statistical analysis

Descriptive statistics were used for data analysis, carried out using the Statistical Package for Social Sciences (SPSS), version 21.0.

## Results

At the time of writing, 104 patients with microcephaly were under evaluation at the AACD in Recife; 78 are still awaiting brain imaging or serology to exclude the other causes of congenital infection. Of the remaining 26 children, two had congenital syphilis and one was born to a mother who was positive for antibodies to HIV. This report therefore includes data on 23 children (10 girls and 13 boys) with presumed congenital Zika virus infection. Dates of birth ranged from July to December 2015. All the children were born in the state of Pernambuco. Cases were seen on a first come first served basis, and not according to severity. All 23 mothers were able to recall whether they had had a rash during pregnancy; 22 reported a rash—17 (77%) in the first trimester, five (23%) in the second trimester, and none in the third trimester.

The head circumference of 20 of the 23 (87%) newborn babies was 2 SD below the mean for sex and gestational age (range 23.0–31.5 cm). Although three children (13%) had a normal head circumference for gestational age and sex, they were included in this report because they met the original criterion for microcephaly (head circumference  $\leq 33$  cm) and had features of congenital infection on brain imaging. One of these children was born preterm (head circumference 29.5 cm) and two were born after 37 weeks (head circumference 33 cm in both). Twenty of the 23 (87%) newborn babies were born at term and 9/23 (39%) were small for gestational age. The anterior fontanelle was closed in 20 (87%) babies at the first clinical examination. Craniofacial

disproportion was present in 18/23 (78%); seven (30%) had an exuberant external occipital protuberance and 12 (52%) a redundant scalp skin. Table 2 shows the individual clinical data for both mothers and infants in all cases of this series.

Six of the 23 children tested positive for IgM antibodies to Zika virus in the cerebrospinal fluid. The other 17 met the protocol criteria for presumed Zika virus related congenital infection but were not tested for IgM antibodies as the test is not yet available on a routine basis. The findings in the six children with positive test results were similar to those of the remaining 17 children who were not tested.

Of the 23 children, 15 underwent CT only, seven both CT and MRI, and one MRI only. All CT scanning was performed without contrast, and only one child underwent MRI with contrast. Tables 3 and 4 present the individual radiological data found in CT and MRI scans, respectively. All except three of the 22 children who underwent CT were reviewed by two experienced neuroradiologists. Information from the three cases not reviewed was provided by radiological report and the clinical neurologist who analysed the images during the children's examination. All data for these three children are described in the tables, except for enlargement of the cisterna magna and the anterior supratentorial subarachnoid space, as this information was not specified in the report or by the neurologist. Two experienced neuroradiologists (MdFVA, AMB-L) reviewed all the MRI scans. One child underwent T2 weighted imaging only; therefore, it was not possible to evaluate the

**Table 2 | Individual clinical data (mother and infant) of 23 children with presumed Zika virus congenital infection**

Patient No	Sex	Age at imaging (days)		Mothers		Infants					
		CT	MRI	Age (years)	Month of pregnancy with rash	Gestational age at birth (weeks)	Phase of microcephaly diagnosis	Head circumference at birth (cm)	Anterior fontanelle	Craniofacial disproportion	Positive for IgM antibodies to Zika virus in CSF
1	Girl	24	-	42	Second	40	Pregnancy	28.5	Closed	Yes	No data
2	Girl	38	129	34	Second	35	Pregnancy	29.5	Closed	No	Positive
3	Girl	11	-	19	Fourth	37	At birth	27	Closed	Yes	Positive
4	Boy	37	6	39	Second	38	Pregnancy	28	Closed	Yes	No data
5	Boy	1	-	26	Sixth	38	Pregnancy	29	Closed	Yes	No data
6	Boy	4	7	34	Second	38	At birth	33	0.5x0.5 cm	No	No data
7	Boy	<1	6	30	Sixth	39	At birth	33	Closed	Yes	No data
8	Girl	104	-	23	Third	36	At birth	27	Closed	Yes	No data
9	Boy	33	-	28	Third	31	Pregnancy	23	Closed	Yes	Positive
10	Boy	1	44	41	Third	37	Pregnancy	27	Closed	Yes	Positive
11	Boy	9	-	35	First	37	Pregnancy	28	Closed	Yes	No data
12	Girl	<1	-	30	Third	39	Pregnancy	26	Closed	Yes	No data
13	Boy	3	-	34	Second	38	Pregnancy	30	2.5x2.5 cm	No	No data
14	Girl	8	-	29	Third	39	At birth	26	Closed	Yes	No data
15	Girl	3	-	27	Fifth	37	Pregnancy	31	Closed	Yes	No data
16	Girl	1	-	30	Second	38	Pregnancy	30	Closed	No	No data
17	Boy	7	-	24	Third	39	At birth	26	Closed	Yes	No data
18	Boy	8	-	37	Third	39	Pregnancy	28	Closed	Yes	No data
19	Boy	12	-	17	No rash	40	At birth	27	Closed	Yes	No data
20	Boy	16	-	27	Third	39	Pregnancy	27	Closed	Yes	No data
21	Girl	33	162	32	Third	37	Pregnancy	30	Closed	Yes	Positive
22	Boy	8	113	26	Fourth	40	Pregnancy	31.5	1.0x1.0 cm	No	Positive
23	Girl	-	8	22	Second	30	Pregnancy	40	Closed	Yes	No data

CT=computed tomography; MRI=magnetic resonance imaging; CSF=cerebrospinal fluid.



Table 3 | Radiological data of 22 children with congenital infection presumed to be caused by Zika virus who underwent computed tomography

Patient No	Decreased brain volume	Location of calcifications							Brainstem hypoplasia	Cerebellum hypoplasia	Enlarged cisterna magna	Enlarged subarachnoid space
		Ventriculomegaly	MCD	Junction between cortical and subcortical white matter	Basal ganglia	Periventricular	Brainstem	Cerebellum				
1	Yes	Yes	Yes	Yes	Yes	No	Yes	No	No	Yes	Yes	Yes
2	Yes*	Yes*	Yes	Yes	No	No	No	No	Yes	No	Yes	No
3	Yes	Yes	Yes	Yes	Yes	No	No	No	No	Yes	No	Yes
4	Yes	Yes	Yes	Yes	Yes	Yes	No	No	No	No	No	Yes
5	Yes	Yes	Yes	Yes	No	Yes	No	No	No	No	No	No
6	Yes	Yes	Yes	Yes	Yes	No	Yes	No	Yes	No	Yes	No
7†	Yes	Yes	Yes	Yes	No	No	No	No	No	No	No data	No data
8	Yes	Yes	Yes	Yes	No	No	No	No	Yes	No	Yes	Yes
9	Yes	Yes	Yes	Yes	Yes	Yes	No	No	Yes	Yes	Yes	Yes
10	Yes	Yes	Yes	Yes	No	Yes	No	No	Yes	Yes	Yes	Yes
11	Yes	Yes	Yes	Yes	Yes	No	Yes	No	No	No	Yes	Yes
12	Yes	Yes	Yes	Yes	Yes	Yes	No	No	No	No	Yes	Yes
13†	Yes	No	Yes	Yes	No	No	No	No	No	No data	No data	No data
14	Yes	Yes	Yes	Yes	Yes	Yes	Yes	Yes	Yes	Yes	Yes	Yes
15	Yes	Yes	Yes	Yes	Yes	No	Yes	No	No	No	Yes	Yes
16†	Yes	Yes	Yes	Yes	Yes	Yes	Yes	No	No	No data	No data	No data
17	Yes	Yes	Yes	Yes	Yes	No	No	No	No	Yes	Yes	Yes
18	No	No	No	Yes	No	No	No	No	No	No	No	No
19	Yes	Yes	Yes	Yes	Yes*	Yes	Yes	Yes	Yes	Yes	Yes	Yes
20	Yes	Yes	Yes	Yes	Yes	Yes	Yes	No	Yes	Yes	Yes	Yes
21	Yes	Yes	Yes	Yes	No	Yes	No	No	Yes	Yes	Yes	Yes
22	No	No	Yes	Yes	No	No	No	No	No	Yes	Yes	No

MCD=malformation of cortical development.

\*Asymmetrical.

†Information provided by radiological report and clinical information given by neurologist.

Table 4 | Radiological data of eight children with congenital infection presumed to be caused by Zika virus who underwent magnetic resonance imaging

Patient No	Decreased brain volume	Simplified gyral pattern	Corpus callosum	Location of calcifications				Brainstem hypoplasia	Cerebellum hypoplasia	Enlarged cisterna magna	Enlarged anterior ST space
				Myelination	Junction between cortical and subcortical white matter	Basal ganglia	Periventricular				
2	Yes*	Yes*	Hypogenesis	Delayed	Yes	No	No	Yes	No	Yes	No
4†	Yes*	No	Normal	Delayed	No data	No data	No data	No	No	No	Yes*
6	Yes	Yes*	Normal	Delayed	Yes	Yes	Yes	Yes	No	Yes	No
7	Yes	Yes	Hypoplasia	Delayed	Yes	No	No	No	No	Yes	Yes
10	Yes	Yes	Hypogenesis	Delayed	Yes	No	Yes	Yes	Yes	Yes	Yes
21	Yes	Yes	Hypogenesis	Delayed	Yes	No	Yes	Yes	No	Yes	Yes
22	Yes†	No	Hypoplasia	Normal	Yes	No	No	No	No	Yes	No
23	Yes	Yes	Hypoplasia	Delayed	Yes	Yes	Yes	No	No	Yes	Yes

MCD=malformation of cortical development; ST=supratentorial subarachnoid.

\*Asymmetrical.

†Calcifications were not assessed because T1 weighted and susceptibility magnetic weighted imaging were not performed.

#Data different from that found by computed tomography probably owing to better sensitivity of magnetic resonance imaging.

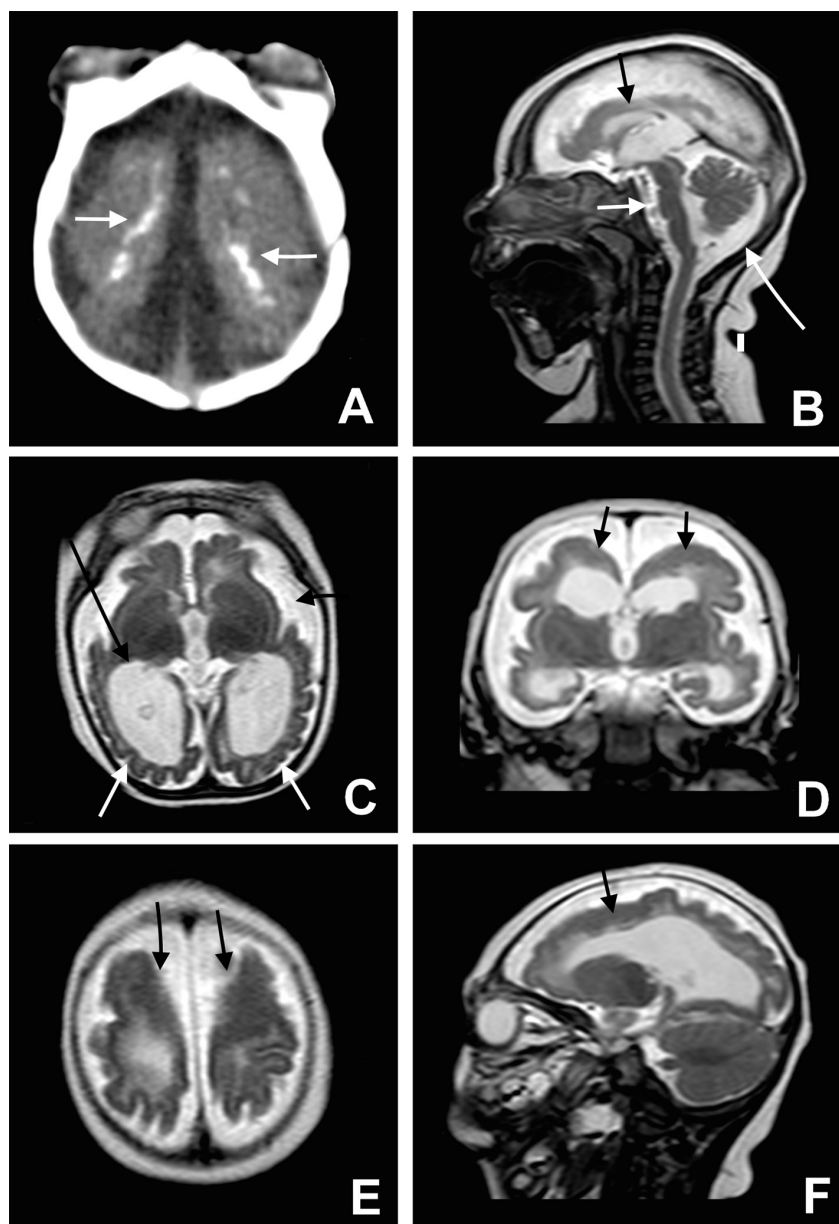


**Fig 2 | Microcephaly, cortical malformation, and brain calcification.** Axial CT image (A) shows many small dystrophic calcifications in the junction between cortical and subcortical white matter (white arrows) and noticeable reduction of the brain parenchyma thickness. Sagittal T2 weighted image (B) shows hypogenesis of the corpus callosum (black arrow), enlarged cisterna magna (long white arrow), and pons hypoplasia (white arrow). Axial T2 weighted image (C) shows simplified gyral pattern (white arrows), ventriculomegaly (long black arrow) widely open Sylvian fissure as well as enlargement of subarachnoid space (black arrow). Coronal T2 weighted image (D) shows pachygyria in the frontal lobes (black arrows). Note the bilateral cortical thickness in the pachygyric frontal lobe (black arrows), shown on axial and sagittal T2 weighted images (E and F)

presence of calcifications on MRI. However, this child had calcifications on CT scans.

The main imaging findings on CT (fig 2A and fig 5A and B) and MRI (fig 2B-F, fig 3A-D, fig 4A-C, and fig 5C-F) were brain calcifications specifically predominant in the junction between cortex and subcortical white matter (fig 2A, fig 3B, fig 4C, and fig 5A-D) associated with malformations of cortical development. The calcifications were mostly punctiform; however, in some cases, linear or even coarse calcifications were also present.

In the children who underwent MRI, the main cortical malformations were a simplified gyral pattern (fig 2C, fig 3B, and fig 4B and C), polymicrogyria (fig 5E), and pachygyria (fig 2D and E). Overall, the malformations were present in the entire brain, especially the simplified gyral pattern (only two of eight children did not present this pattern). However, in all of the children the frontal lobe was among the lobes most affected, especially by polymicrogyria and pachygyria. Other malformations found were hemimegalencephaly and periventricular heterotopic grey matter.

Other findings were ventriculomegaly (fig 2C, D, and F, and fig 3B-D), an enlarged cisterna magna (fig 2B, fig 3A, fig 4A, and fig 5F), abnormalities of the corpus callosum (hypoplasia or hypogenesis) (fig 2B, fig 3A, fig 4A, and fig 5F), cerebellar and brainstem hypoplasia (fig 2B and fig 3A), and an enlarged supratentorial subarachnoid space (fig 2C and D, and fig 3C). Tables 5 and 6 present the results of the descriptive analysis of the qualitative variables found on the CT and MRI scans, respectively. Table 7 illustrates the classification and location of malformations found on the MRI scans.

## Discussion

In this paper we describe the characteristic findings from brain imaging (computed tomography (CT) and magnetic resonance imaging (MRI)) in children with presumed Zika virus related congenital infection during the Brazilian microcephaly epidemic. Calcifications located predominantly in the junction between cortical and subcortical white matter areas were observed in all the children, whereas intraparenchymal cysts were not detected in any of them. All the children showed malformations of cortical development and sulcation. A common observation was microcephaly with a simplified pattern of cortical circulations with normal cortical thickness, associated with areas of thick cortex (polymicrogyria or pachygyria) predominantly located in the frontal lobes. Decreased brain volume, evaluated by qualitative visual inspection, was a common finding, and ventriculomegaly was present in all the children, with a predominant enlargement of the posterior portions of the lateral ventricles (trigone and posterior horn of lateral ventricles). Abnormalities of the corpus callosum (hypogenesis and hypoplasia) and delayed myelination were also common. Interestingly, the cisterna magna was enlarged in most of the cases, with or without cerebellar hypoplasia. Some of the children showed a symmetrical enlargement of the anterior subarachnoid space of the supratentorial compartment, invariably associated with severe ventriculomegaly.

We present the largest and more detailed case series of neuroimaging findings in children with microcephaly and presumed Zika virus related infection. Some, but not all, of our findings are in line with previous reports. An autopsy study of congenital infection in a brain sample of a 32 week old aborted fetus (due to termination of the pregnancy) with confirmed reverse transcriptase-polymerase chain reaction for Zika virus described the presence of microcephaly, almost complete agyria, widely open Sylvian fissures, a small

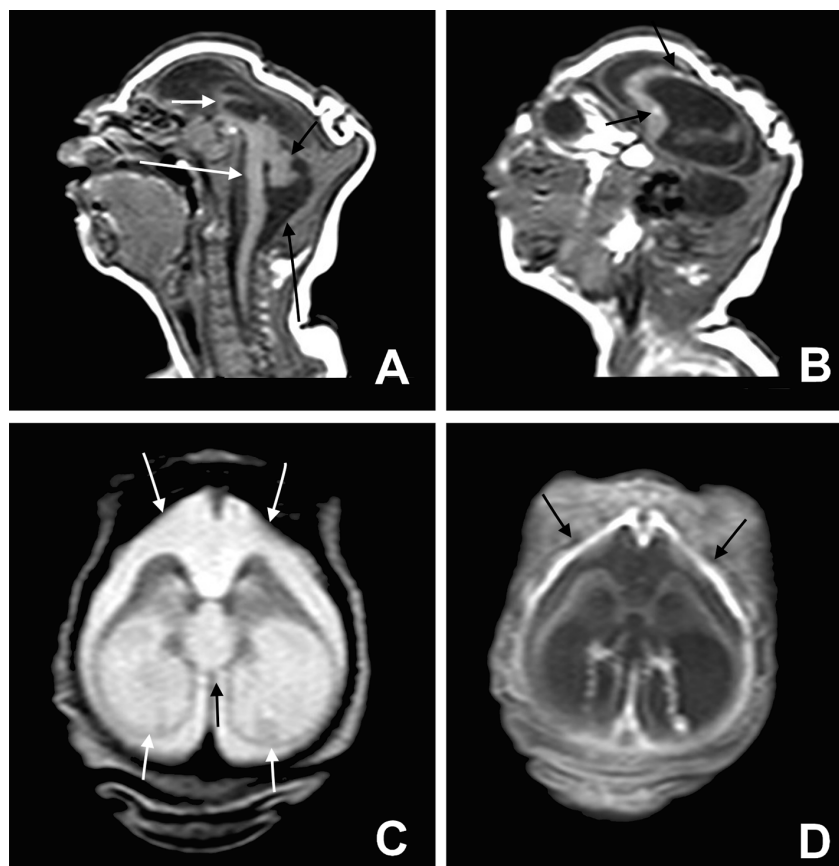


**Fig 3 | Severe microcephaly.** Sagittal T1 weighted image (A) shows a profound craniofacial disproportion, noticeably hypogenetic corpus callosum (short white arrow), and brainstem (long white arrow) and cerebellum hypoplasia (short black arrow). In addition, the cisterna magna is enlarged (long black arrow). Observe the small dystrophic calcifications hyperintense on T1 weighted image (B) in the frontal lobe (black arrows) and extremely simplified gyral pattern. Axial T2 weighted image (C) shows severe ventriculomegaly, mainly at the posterior horn and ventricular atrium (short white arrows). Note the bulging walls of the ventricle, the upward dilated third ventricle (black arrow), and enlargement of the subarachnoid space (long white arrows). Axial T1 weighted image fat suppression post-contrast (D) shows thickness and enhancement of frontal pachymeningitis (black arrows). These last findings (C and D) may indicate a blockage in the cerebrospinal fluid pathways and/or reduced absorption of cerebrospinal fluid owing to impairment of the meninges or injury of arachnoid granulations

cerebellum and brainstem, and enlarged lateral ventricles.<sup>3</sup> Numerous cortical and subcortical white matter calcifications of various sizes were also seen in the frontal, parietal, and occipital lobes. In a recent report of the neuroimaging features (on CT and transfontanellar cranial ultrasound scans) of 27 children with presumed Zika virus related congenital infection and microcephaly, calcification was present in 74% of the children, ventricular enlargement in 44%, and neuronal migration disorders in 33%.<sup>18</sup> However, no CT nor ultrasound images were shown in this report. In contrast to what we found, periventricular calcifications were one of the most common features in that series.<sup>18</sup> This may be due to the difficulty in differentiating the site of the calcifications, as the ventricles are enlarged and the cerebral parenchyma is thin, making the cortical and subcortical white matter calcifications appear periventricular. This problem was potentially minimised in our study because the thin parenchyma could be better visualised in the MRI cases, and this enabled us to better identify the exact localisation of the majority of the calcifications in the junction between cortical and subcortical white matter. This also led to a more careful evaluation of the true location of calcifications during the retrospective review of CT images in our study.

Several features found in children with presumed Zika virus related infection are similar to those encountered in congenital infections of the central nervous system due to other agents such as *Toxoplasma gondii*, cytomegalovirus, rubella, and herpes simplex virus (TORCH), including decreased brain volume, ventriculomegaly, malformations of cortical development, and simplified gyral pattern, delayed myelination, and cerebellar hypoplasia.<sup>20,21</sup> Table 8 compares the major neuroimaging features of TORCH infections,<sup>20</sup> and the characteristics of imaging findings in children with presumed Zika virus related congenital infection.

Intracranial calcifications, present in all the children in our study, are an important feature of congenital central nervous system infection but they are also seen in other genetic and metabolic diseases.<sup>22</sup> The pattern

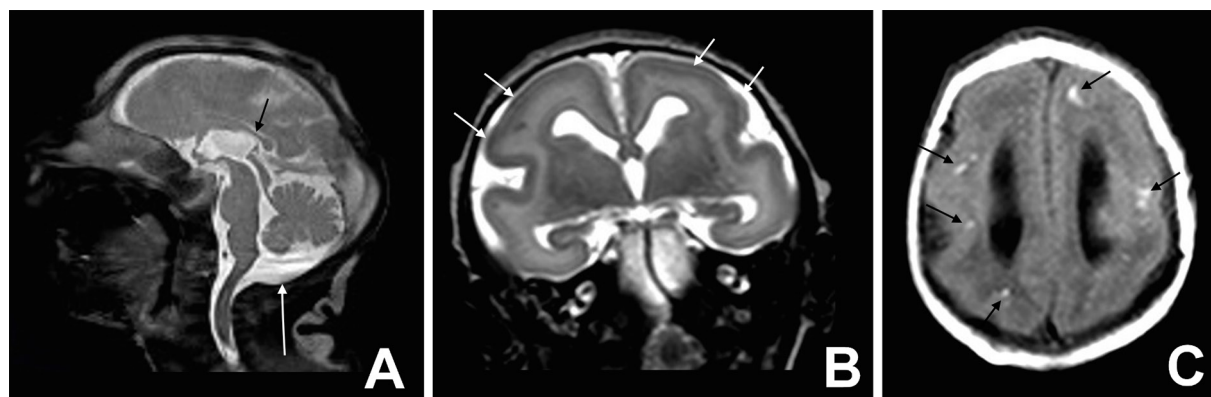
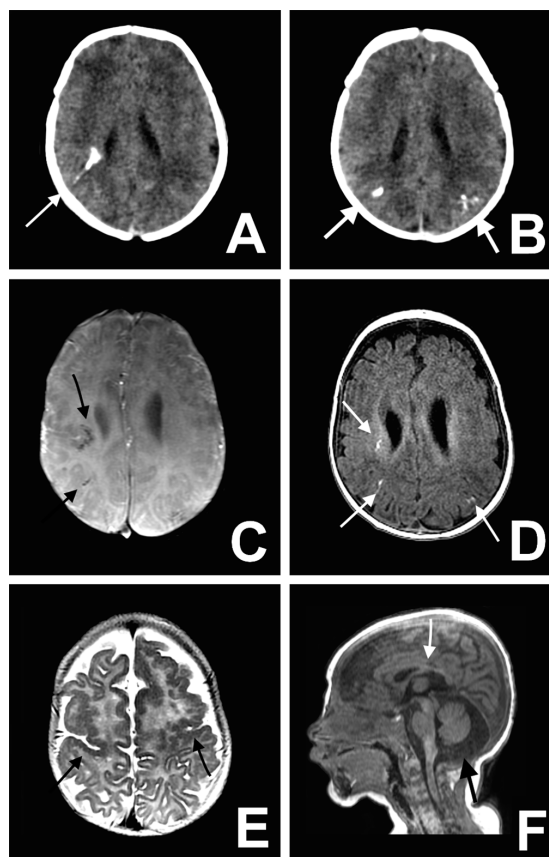


**Fig 4 | Microlissencephaly.** Sagittal T2 weighted image (A) and axial T2 weighted image (B) show moderate microcephalic brain, almost completely smooth cerebral surface with a thick cortex (short white arrows), and hypoplasia of corpus callosum (black arrow). In addition, the cisterna magna (long white arrow) is enlarged. Axial T1 weighted image (C) shows multiple hyperintense subcortical punctate dystrophic calcifications (black arrows)



**Fig 5 | Mild microcephaly.** Axial non-contrast CT image (A and B) shows multiple bilateral calcifications in the junction between cortical and subcortical white matter (white arrows). Axial susceptibility magnetic weighted image (C) shows multiple foci of T2-hypointensity in subcortical frontal white matter (black arrows), and axial T1 weighted image (D) shows linear or punctiform foci of T1-shortening (white arrows), which correspond to the calcifications on CT. Axial T2 weighted image (E) shows bilateral frontal and central sulcus polymicrogyria (black arrows). Note the thickened and irregular cortical-white matter junction. Sagittal T1 weighted image (F) shows enlarged cisterna magna (black arrow) and hypoplastic corpus callosum (white arrow)



and location of calcifications and other abnormalities can suggest a possible cause. For example, calcifications in periventricular areas is more common in congenital infection related to cytomegalovirus.<sup>20 21</sup> Another characteristic that may suggest cytomegalovirus as the causal agent in a microcephalic child is the presence of temporal and germinal zone cysts.<sup>20</sup> In our series, calcification was found most often at the junction between cortical and subcortical white matter, and intraparenchymal cysts were not observed in any of the children in our study.

Although CT has been the mainstay of imaging for intracranial calcification for many years and remains superior for identification and delineation, we were

**Table 5 | Descriptive analysis of qualitative variables found on computed tomography brain scans in 22 children with presumed Zika virus related microcephaly**

Variables	No (%) of children
Location of calcifications:	22 (100)
Junction between cortical and subcortical white matter	22 (100)
Basal ganglia	13 (59)
Periventricular	10 (45)
Brainstem	8 (35)
Cerebellum	11 (50)
Decreased brain volume	20 (91)
Malformations of cortical development	21 (95)
Ventriculomegaly	19 (86)
Cerebellum or brainstem hypoplasia	11 (50)

**Table 6 | Descriptive analysis of qualitative variables found on magnetic resonance imaging brain scans in eight children with presumed Zika virus related microcephaly**

Variables	No (%) of children
Location of calcifications*:	7
Junction between cortical and subcortical white matter*	7
Basal ganglia*	2 (29)
Cerebellum*	0 (0)
Brainstem*	1 (14)
Decreased brain volume:	8 (100)
Mild	2 (25)
Moderate or severe	6 (75)
Malformations of cortical development	8 (100)
Most affected lobes:	
Frontal	8 (100)
Insula	4 (50)
Parietal	3 (38)
Temporal	2 (25)
Occipital	1 (13)
Simplified gyral pattern	6 (75)
Ventriculomegaly	8 (100)
Corpus callosum abnormalities:	6 (75)
Hypogenetic	3 (38)
Hypoplastic	3 (38)
Cerebellum or brainstem hypoplasia	3 (38)
Enlarged cisterna magna	7 (88)
Delayed myelination	7 (88)
Symmetry of findings	6 (75)
Enlarged subarachnoid supratentorial space	3 (38)

\*One patient not analysed owing to absence of T1 weighted and susceptibility magnetic weighted imaging.

able to detect calcifications on MRI. Interestingly, in our series the calcifications were seen as hyperintense on T1 weighted images and hypointense on susceptibility magnetic weighted images. Besides calcifications, these types of signal can also indicate, for example, methaemoglobin, manganese deposition, melanin, and lipid on T1 weighted images;<sup>22 23</sup> iron deposition, deoxyhaemoglobin, hemosiderin/ferritin on T2\* weighted<sup>22 23</sup> and susceptibility magnetic weighted images;<sup>24</sup> and small veins in susceptibility magnetic weighted images.<sup>24</sup> Among all MRI techniques, susceptibility magnetic weighted imaging was found to increase the sensitivity of MRI to intracranial calcifications considerably.<sup>22</sup> Of the eight patients who underwent MRI, seven also underwent CT scan; the punctate images observed on MRI scans corresponded to the calcifications seen on CT scans in all of them. Hyper-hydrated calcium in a brain not yet myelinated can explain the appearance on the T1 weighted scans.<sup>22</sup>

Some genetic disorders have imaging features similar to those seen in children with congenital infections. Aicardi-Goutières syndrome and RNASET2 related disease show brain calcifications, and the latter also presents with cysts in temporal lobe, but cortical malformations (common in all the children in our study) have not been described in these conditions.<sup>22</sup> Another genetic disease, band-like calcification with simplified gyration and polymicrogyria, presents a characteristic pattern of symmetrical continuous or



**Table 7 | Classification of malformations found on magnetic resonance imaging of brain**

Patient No	Month of pregnancy with rash	Classification of malformations of cortical development	Grade of decrease in brain volume*
1	Second†	Focal left frontal cortical polymicrogyria	I
2	Second†	Right frontal and perisylvian polymicrogyria	II
3	Second†	Right hemimegalencephaly and polymicrogyria; left pachygyria	III
4	Second	Bilateral pachygyria predominant in frontal and temporal lobes	II
5	Third	Bilateral superior frontal gyri pachygyria	III
6	Third	Bilateral lissencephaly	III
7	Fourth	Bilateral frontal and perisylvian polymicrogyria	I
8	Sixth	Bilateral frontal and perisylvian polymicrogyria	II

\*Classification of graduation of brain volume according to visual inspection: I=mild; II=moderate; III=severe.

†All three patients with asymmetrical cortical malformations were presumably infected in second month of pregnancy, which corresponds to period of mother's rash.

semicontinuous ribbon of cortical calcification,<sup>22</sup> which was not found in the children in our study.

Unlike the situation with other congenital infections, children with presumed Zika virus related infection had cortical malformations (pachygyria and polymicrogyria) located predominantly in the frontal lobes. This frontal predominance has not been described in other congenital infections of the central nervous system. The presence of cortical malformations can help differentiate Zika virus related congenital infection from toxoplasmosis, as malformations of cortical development are uncommon in the latter.<sup>20</sup>

An enlarged cisterna magna ( $\geq 10$  mm on midsagittal images)<sup>25</sup> was a common finding, even in children with no signs of cerebellar hypoplasia. A similar finding was reported in the fetus of a mother who had symptoms compatible with Zika virus infection.<sup>2</sup> This finding can be identified in cytomegalovirus related congenital infection, but was not common, as described by two studies using ultrasound in 3/8 and 4/8 of fetuses.<sup>26,27</sup>

The brain damage caused by Zika virus infection in these children was extremely severe, indicating a poor

prognosis for neurological function. This scenario might be the worse one in the disease severity spectrum. Less severe or mild forms of the disorder may proceed without microcephaly, but may present microencephaly without clinically significant diminution of the head size. The initial selection of 33 cm as the threshold for head circumference was based on this assumption, but this resulted in an alarming increase in the number of "microcephalic" children, probably including ones without congenital infection. Thus, a new head circumference criterion of 32 cm or less was determined.

Zika virus related microcephaly may occur in the absence of any apparent infectious disease during the course of a pregnancy, as Zika virus infection is known to be asymptomatic in three of every four infected patients.<sup>13</sup> Additionally, it is important to understand that the disease is not microcephaly, but a new congenital infection presumed to be related to Zika virus (that is, Zika virus congenital syndrome), which can include microcephaly and other malformations. Furthermore, some patients presented an enlarged supratentorial subarachnoid space, which can make the head circumference appear to be bigger than the actual brain volume, thereby masking a small brain.

#### Strengths and weaknesses of this study

Our study has several limitations. The images were acquired using different scanners, but these devices were of similar technical capabilities and almost all the images were reviewed by the same neuroradiologists. The severity of microcephaly and the age of the children sometimes made it difficult to interpret the small brain structures on the scans. Only a third of the children in our study underwent MRI, mainly because of costs and because this procedure was not in the Brazilian Ministry of Health protocol, being performed only when indicated. Although MRI is less sensitive than CT for calcifications, in the children in this study most of the calcifications were identified in T1 weighted or susceptibility magnetic weighted images, or both.

**Table 8 | Major neuroimaging features of TORCH\* infections, according to Barkovich and Raybaud,<sup>20</sup> and proposed characteristics of congenital infection of presumed Zika virus related infection**

Agent	Malformations of cortical development	Location of calcifications	Additional findings
Cytomegalovirus	Lissencephaly with a thin cortex,† polymicrogyria‡	Periventricular (most common), subcortical white matter	Ventriculomegaly, cerebellar hypoplasia, delayed myelination, anterior temporal lobe and germinal zone cysts, diffuse or multifocal white matter abnormalities
<i>Toxoplasma gondii</i>	Macrocephaly or microcephaly (uncommon)	Basal ganglia, periventricular, cortex, subcortical white matter	Hydrocephalus, ventriculomegaly, areas of porencephaly
Rubella virus	Microcephaly	Periventricular, basal ganglia, brainstem (uncommon)	Ventriculomegaly, delayed myelination, periventricular and basal ganglia cysts, frontal dominant white matter lesions
Herpes simplex virus	Microcephaly with cortical thinning	Gyral (late stages)	Ventriculomegaly, multifocal areas of grey matter and white matter abnormalities, multicystic brain, haemorrhage, encephalomalacia, watershed pattern of injury
Presumed Zika virus	Microcephaly with simplified gyral pattern; lissencephaly or polymicrogyria (mainly frontal)	Junction between cortical and subcortical white matter (most common); basal ganglia, periventricular	Ventriculomegaly (mainly in the posterior portions of the lateral ventricles), enlarged cisterna magna, abnormalities of the corpus callosum (hypoplasia or hypogenesis), delayed myelination, cerebellar and brainstem hypoplasia

\*Toxoplasma, other viruses, rubella, cytomegalovirus, and herpes virus.

†Onset at beginning of second trimester.

‡Onset in middle of second trimester.

Another limitation of this study is that no routinely available test exists for definitive confirmation of the Zika virus; for this reason, in most cases the diagnosis was established by clinical and radiological criteria and exclusion of other congenital infections. In addition, epidemiological support for the diagnosis—the mothers' rash during pregnancy—was based exclusively on the mothers' recall.

This study shows the largest and most detailed case series of neuroimaging findings in children with microcephaly and presumed Zika virus related infection to date.

## Conclusions

We have described the imaging (CT and MRI) findings in a series of children with presumed Zika virus related congenital infection, which in most of the cases show severe cerebral damage. The imaging features most often found were calcifications in the junction between cortical and subcortical white matter associated with malformations of cortical development, often with a simplified gyral pattern and predominance of pachygyria or polymicrogyria in the frontal lobes. Additional findings were an enlarged cisterna magna, corpus callosum abnormalities (hypoplasia or hypogenesis), ventriculomegaly, delayed myelination, and cerebellum and brainstem hypoplasia.

We thank anesthesiology staff Antonio Monteiro and Cristovam A de Lira Terceiro, magnetic resonance imaging technician Edineide Cristina Leite Lopes, and the Centro Diagnostico Multimagem for their help.

**Contributors:** All authors contributed to the clinical (VvdL, RRC, MAR, PSdS, MDCGdC, AvdL) or radiological (MdFVA, AMB-L) assessment, according to their own specialty, to the concept and design of the study, to analysis and interpretation of the data, and to the draft of the final version of the manuscript (MdFVA, VvdL, AMB-L, ACDH, MMV). MdFVA is the guarantor.

**Funding:** This study received no external funding.

**Competing interests:** All authors have completed the ICMJE uniform disclosure form at [www.icmje.org/coi\\_disclosure.pdf](http://www.icmje.org/coi_disclosure.pdf) and declare: no support from any organisation for the submitted work; no financial relationships with any organisations that might have an interest in the submitted work in the previous three years; no other relationships or activities that could appear to have influenced the submitted work.

**Ethical approval:** The investigations were conducted in accordance with the emergency clinical protocol of the Brazilian Ministry of Health.

**Data sharing:** Additional information is available on request from the corresponding author ([fatima.vascoaragao@gmail.com](mailto:fatima.vascoaragao@gmail.com)).

**Transparency:** The lead author (MdFVA) affirms that the manuscript is an honest, accurate, and transparent account of the study being reported; that no important aspects of the study have been omitted; and that any discrepancies from the study as planned have been explained.

This is an Open Access article distributed in accordance with the Creative Commons Attribution Non Commercial (CC BY-NC 3.0) license, which permits others to distribute, remix, adapt, build upon this work non-commercially, and license their derivative works on different terms, provided the original work is properly cited and the use is non-commercial. See: <http://creativecommons.org/licenses/by-nc/3.0/>.

- 1 Ministério da Saúde (Brazil). Protocolo de vigilância e resposta à ocorrência de microcefalia. 2016 Jan 22 [cited 2016 Feb 20]. In: Ministério da Saúde (Brazil). <http://portalsaude.saude.gov.br/images/pdf/2016/janeiro/22/microcefalia-protocolo-de-vigilancia-e-resposta-v1-3-22jan2016.pdf>.
- 2 Oliveira Melo AS, Malinger G, Ximenes R, Szejnfeld PO, Alves Sampaio S, Bispo de Filippis AM. Zika virus intrauterine infection causes fetal brain abnormality and microcephaly: tip of the iceberg? *Ultrasound Obstet Gynecol* 2016;47:6-7. doi:10.1002/uog.15831.

- 3 Mlakar J, Korva M, Tul N, et al. Zika virus associated with microcephaly. *N Engl J Med* 2016;374:951-8. doi:10.1056/NEJMoa1600651.
- 4 Bell TM, Field EJ, Narang HK. Zika virus infection of the central nervous system of mice. *Arch Gesamte Virusforsch* 1971;35:183-93. doi:10.1007/BF01249709.
- 5 Tang H, Hammack C, Ogden SC, et al. Zika virus infects human cortical neural progenitors and attenuates their growth. *Cell Stem Cell* 2016;18:1-4. PMID:26952870.
- 6 Brasil P Jr, Pereira JP Jr, Raja Gabaglia C, et al. Zika virus infection in pregnant women in Rio de Janeiro – Preliminary report. *N Engl J Med* 2016; published online 4 Mar. doi:10.1056/NEJMoa1602412.
- 7 Duffy MR, Chen TH, Hancock WT, et al. Zika virus outbreak on Yap Island, Federated States of Micronesia. *N Engl J Med* 2009;360:2536-43. doi:10.1056/NEJMoa0805715.
- 8 Mackenzie JS, Gubler DJ, Petersen LR. Emerging flaviviruses: the spread and resurgence of Japanese encephalitis, West Nile and dengue viruses. *Nat Med* 2004;10(Suppl):S98-109. doi:10.1038/nm1144.
- 9 Morens DM, Folkers GK, Fauci AS. The challenge of emerging and re-emerging infectious diseases. *Nature* 2004;430:242-9. doi:10.1038/nature02759.
- 10 Sips GJ, Wilschut J, Smit JM. Neuroinvasive flavivirus infections. *Rev Med Virol* 2012;22:69-87. doi:10.1002/rmv.712.
- 11 Dick GW, Kitchen SF, Haddock AJ. Zika virus. I. Isolations and serological specificity. *Trans R Soc Trop Med Hyg* 1952;46:509-20. doi:10.1016/0035-9203(52)90042-4.
- 12 Hayes EB. Zika virus outside Africa. *Emerg Infect Dis* 2009;15:1347-50. doi:10.3201/eid1509.090442.
- 13 Besnard M, Lastere S, Teissier A, Cao-Lormeau V, Musso D. Evidence of perinatal transmission of Zika virus, French Polynesia, December 2013 and February 2014. *Euro Surveill* 2014;19:1-4. doi:10.2807/1560-7917.ES2014.19.13.20751.
- 14 Campos GS, Bandeira AC, Sardi SI. Zika virus outbreak, Bahia, Brazil. *Emerg Infect Dis* 2015;21:1885-6. doi:10.3201/eid2110.150847.
- 15 Centre d'hygiène et de salubrité publique de la Direction de la santé. Bulletin téléchargeable sur les sites suivants: Réseau Océanien de Surveillance de Santé Publique. 2015 Nov 24 [cited 2016 Feb 20]. In: Centre d'hygiène et de salubrité publique de la Direction de la santé. [www.hygiene-publique.gov.pf/spip.php?article120](http://www.hygiene-publique.gov.pf/spip.php?article120).
- 16 Tavernise S, McNeil DG Jr. Zika virus a global health emergency, WHO says. 2016 Feb 1 [cited 2016 Feb 20]. In: *New York Times*. [www.nytimes.com/2016/02/02/health/zika-virus-world-health-organization.html?\\_r=0](http://www.nytimes.com/2016/02/02/health/zika-virus-world-health-organization.html?_r=0).
- 17 Ministério da Saúde (Brazil). Monitoramento dos casos de microcefalia no Brasil. Informe epidemiológico nº 13. 2016 Feb 13 [cited 2016 Feb 20]. In: Centro de Operações de Emergências em Saúde Pública sobre Microcefalias. <http://portalsaude.saude.gov.br/images/pdf/2016/fevereiro/17/coes-microcefalia-inf-epi-13-se06-2016.pdf>.
- 18 Schuler-Faccini L, Ribeiro EM, Feitosa IML, et al. Brazilian Medical Genetics Society–Zika Embryopathy Task Force. Possible association between Zika virus infection and microcephaly – Brazil, 2015. *MMWR Morb Mortal Wkly Rep* 2016;65:59-62. [www.cdc.gov/mmwr/volumes/65/wr/mm6503e2.htm](http://www.cdc.gov/mmwr/volumes/65/wr/mm6503e2.htm)doi:10.15585/mmwr.mm6503e2.
- 19 Martin DA, Muth DA, Brown T, Johnson AJ, Karabatsos N, Roehrig JT. Standardization of immunoglobulin M capture enzyme-linked immunosorbent assays for routine diagnosis of arboviral infections. *J Clin Microbiol* 2000;38:1823-6. PMID:10790107.
- 20 Barkovich AJ, Raybaud C. *Pediatric neuroimaging*. 5th ed. Lippincott Williams & Wilkins, 2012.
- 21 Sze G, Lee SH. Infectious disease. In: Lee SH, Rao KCVG, Zimmerman RA, eds. *Cranial MRI and CT*. 4th ed. Mc Graw-Hill, 1999: 453-517.
- 22 Livingston JH, Stivaros S, Warren D, Crow YJ. Intracranial calcification in childhood: a review of aetiologies and recognizable phenotypes. *Dev Med Child Neurol* 2014;56:612-26. doi:10.1111/dmcn.12359.
- 23 Hess CP, Purcell DD. Analysis of density, signal intensity and echogenicity. In: Naidich TP, Castillo M, Cha S, Smirniotopoulos JG, eds. *Imaging of the brain*. 1st ed. Saunders, 2013: 45-66.
- 24 Haacke EM, Mittal S, Wu Z, Neelavalli J, Cheng YCN. Susceptibility-weighted imaging: technical aspects and clinical applications, part 1. *AJNR Am J Neuroradiol* 2009;30:19-30. doi:10.3174/ajnr.A1400.
- 25 Bosemani T, Orman G, Boltshauser E, Tekes A, Huisman TA, Poretti A. Congenital abnormalities of the posterior fossa. *Radiographics* 2015;35:200-20. doi:10.1148/rg.351140038.
- 26 Dogan Y, Yuksel A, Kalelioglu IH, Has R, Tatli B, Yildirim A. Intracranial ultrasound abnormalities and fetal cytomegalovirus infection: report of 8 cases and review of the literature. *Fetal Diagn Ther* 2011;30:141-9. doi:10.1159/000330636.
- 27 Malinger G, Lev D, Zahalka N, et al. Fetal cytomegalovirus infection of the brain: the spectrum of sonographic findings. *AJNR Am J Neuroradiol* 2003;24:28-32.p.

© BMJ Publishing Group Ltd 2016